CENTER FOR
MACHINE PERCEPTION

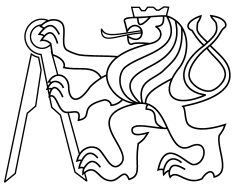

CZECH TECHNICAL
UNIVERSITY

RESEARCH REPORT

ISSN 1213-2365

Recognition of Breathing Pattern by a Photogrammetric Method

(Version 1.1)

Jiří Čihák[1], Jiří Čumpelík[2],
Ladislav Krtička[1], Vladimír Smutný[1],
Pavel Strnad[3], Radim Šára[1],
František Véle[3], Michaela Veverková[4],
Vít Zýka[1]

sara@cmp.felk.cvut.cz

[1] Faculty of Electrical Engineering, Czech Technical University Prague
[2] National Theatre Prague
[3] Faculty of Sports, Charles University Prague
[4] Faculty Hospital Vinohrady, Charles University Prague

CTU–CMP–2005–32

(revision from January 30, 2006)

Available at
ftp://cmp.felk.cvut.cz/pub/cmp/articles/sara/Cihak-TR-2005-32.pdf

This research has been supported by the Grant Agency of the Ministry of Health of the Czech Republic under Project No. NK7735-3/2003.

Research Reports of CMP, Czech Technical University in Prague, No. 32, 2005

Published by

Center for Machine Perception, Department of Cybernetics
Faculty of Electrical Engineering, Czech Technical University
Technická 2, 166 27 Prague 6, Czech Republic
fax +420 2 2435 7385, phone +420 2 2435 7637, www: http://cmp.felk.cvut.cz

Recognition of Breathing Pattern by a Photogrammetric Method

J. Čihák J. Čumpelík L. Krtička V. Smutný P. Strnad
R. Šára F. Véle M. Veverková V. Zýka

(revision from January 30, 2006)

Abstract

A method is proposed that recognizes breathing pattern of a person from a set of image acquired by a photogrammetric system. Special markers are placed on a set of anatomical points over the torso and their 3D position is measured by the system to $\pm 0.1\,\mathrm{mm}$ accuracy. One set of positions is measured in inspiration and one in expiration. The difference of marker positions captures information about the mechanics of breathing motion. A probabilistic index is proposed to recognize three types of breathing pattern according to Kapandji: bucket handle, pump handle and abdominal. The index is used to quantify changes in three sets of individuals after exercise program designed to improve breathing pattern.

Contents

1 Method

1.1 Photogrammetric System

A system has been designed [1] that measures a set of reference points on the body. The system consists of six calibrated cameras, four of them viewing the ventral side of thorax and two of them viewing the dorsal thorax. The reference points are flat coded markers sticked on the skin, see Fig. 1. Since each of the markers is visible in at least two cameras, its three-dimensional position can be determined by triangulation which is a standard photogrammetric method. The accuracy of the system is about 0.1 mm for marker viewing angles up to 72°. A full description of the image acquisition system, automatic marker detection and reading, the 3D position calculation and error analysis of the system is found in [1].

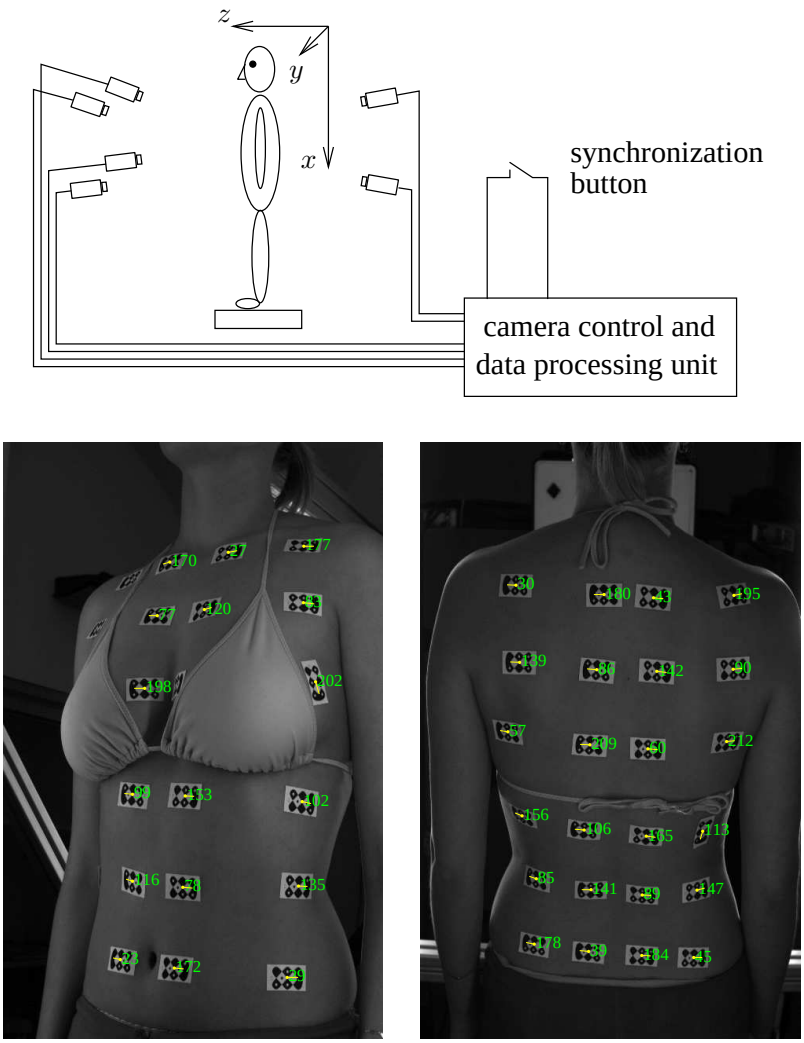

Figure 1: Experimental System Setup. Four anterior digital cameras view the subject from front and two posterior cameras from behind to locate the markers (top). The coordinate system is fixed by the device as shown. Markers are located and their code read by a software system (bottom, the numbers are in internal coding of the system). From their image positions the 3D position is calculated by triangulation. See [1] for details.

A similar system, ELITE, has been described in the literature [2]. Our system differs in using flat markers that sit directly on the skin, which implies they are more stable under vibrations and constrain the subject less.

Image acquisition is controlled by a manual synchronization button. A specialist determines

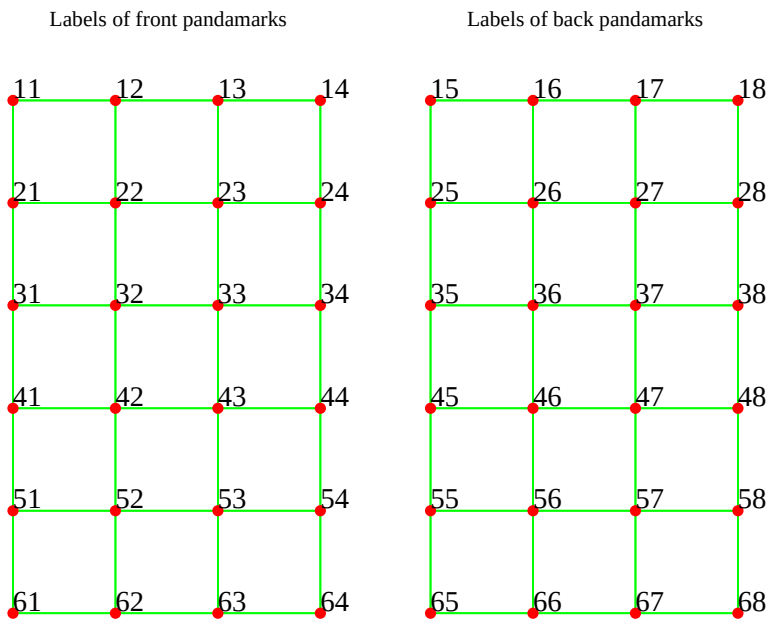

Figure 2: The reference point user coding system. Anterior side (left) and posterior side (right).

the moments of maximum inspiration and maximum expiration of the freely breathing subject. At the moment she presses the synchronization button that triggers image capture (6 images). The subject is standing upright with no additional stabilization or support (except visual) and is instructed to breathe deeply. We experimented with different breathing conditions: normal breathing, deep breathing and breathing after exercise (a 2-floor staircase run). Full analysis is under way but for the sake of this study we selected deep breathing that showed relatively good repeatability.

1.2 Reference Points

The reference points were arranged in six horizontal lines, each line consisting of four points on each body side. They are referred to by their user code in the form ij, where $i = 1, 2, \ldots, 6$ is the horizontal line index and $j = 1, 2, \ldots, 8$ is their horizontal position index. The placement is apparent from Fig. 1 and their coding from Fig. 2. Their anatomical locations were selected as follows:

On the ventral side, vertical lines $j = 2, 3$ are sternoclavicular joint lines and vertical lines $j = 1, 4$ are acromioclavicular joint lines. On the dorsal size, the inner vertical lines are costovertebral joint lines and the outer vertical lines are at spina scapulae mean lines for $i = 1, 2, 3$ and lines at half crista iliaca for $i = 4, 5, 6$.

All lines $i = 1, \ldots, 6$ are horizontal, their horizontality is determined by a laser level. On the ventral side the first horizontal line $i = 1$ is determined by sternoclavicular joint and the second horizontal line $i = 2$ by 2nd rib. In men, line $i = 3$ is defined at half distance between 2nd rib and processus xiphoideus, line $i = 4$ is at processus xiphoideus, and line $i = 5$ at half distance between processus xiphoideus and navel. In women, line $i = 3$ is at half distance between 2nd rib and the inframammalis line, line $i = 4$ is the inframammalis line, and line $i = 5$ is at the half distance between inframammalis line to navel. The line $i = 6$ is the navel line for both men and women.

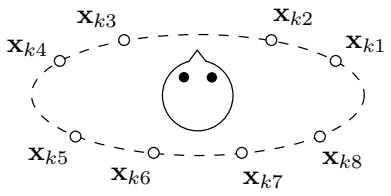

Figure 3: The k-th line of reference points gives a single center of gravity $\mathbf{x}_k$.

1.3 The Normalized Measurement

The coordinate system of the photogrammetric device was defined as follows: The x is the superio-inferior axis (negative values correspond to upward motion), the y is the latero-lateral axis (negative values correspond to leftward motion), and the z is the posterio-anterior axis (negative values correspond to backward motion).

As described above, the k-th of the six lines consists of eight reference points whose spatial position is $\mathbf{x}_{kj}$, $j = 1, 2, \ldots, 8$, as illustrated in Fig. 3. The raw data undergo two normalization steps. First the median

$$\mathbf{x}_m = \frac{1}{2}(\mathbf{x}_{66} + \mathbf{x}_{67}) \tag{1}$$

is subtracted from all measurements

$$\mathbf{x}^*_{ij} = \mathbf{x}_{ij} - \mathbf{x}_m. \tag{2}$$

This step removes most non-breathing motions. The usual magnitude of this motion is about 5mm, which is comparable to breathing motions.

The subject was instructed to perform deep breathing. Normalized reference point positions in maximum inspiration $\mathbf{x}^*_{kj}(i)$ and the position in maximum expiration $\mathbf{x}^*_{kj}(e)$ are obtained. Then, respective centers of gravity for line k are computed as

$$\mathbf{x}_k(i) = \frac{1}{8}\sum_{j=1}^{8} \mathbf{x}^*_{kj}(i) \quad \text{and} \quad \mathbf{x}_k(e) = \frac{1}{8}\sum_{j=1}^{8} \mathbf{x}^*_{kj}(e).$$

For each of the k lines the mean difference vectors over all repeated measurements

$$d\mathbf{x}_k = \mathbf{P}\big(\mathbf{x}_k(i) - \mathbf{x}_k(e)\big)$$

are determined, where

$$\mathbf{P} = \begin{bmatrix} 1 & 0 & 0 \\ 0 & 0 & 1 \end{bmatrix} \tag{3}$$

is a projection matrix that removes the y coordinate (latero-lateral direction, see Fig. 1). The set of 2-dimensional vectors $d\mathbf{x}_k$ for $k = 1, 2, \ldots 6$ is represented by 12 numbers. Finally, the vector $d\mathbf{x}_k$ is normalized by dividing it by the square root of the sum

$$s^2 = \sum_{k=1}^{6}\sum_{i=1}^{3} x_k^2(i), \tag{4}$$

where $x_k(i)$ is the i-th component of vector $\mathbf{x}_k$. The normalization removes the influence of unequal inspiration depth and the difference in individual anatomical sizes. The final normalized measurement is then a 6-column, 2-row matrix

$$\mathbf{X} = \left[\frac{d\mathbf{x}_k}{s}\right]_{k=1}^{6}. \tag{5}$$

1.4 Breathing Prototypes

The composed index we propose in this paper is based on the analysis of prototypical breathing motions performed by a trained subject. To this end, three breathing types were performed repeatedly by the subject. For each breathing type the mean and standard deviation over all inspiration-expiration pairs and all the repeated trials was computed. The resulting normalized prototypes are shown in Tab. 1.

The prototypic breathing types, according to Kapandji [3], were the *bucket handle* breathing, *abdominal* breathing, and the *pump handle* breathing. By analyzing results in Tab. 1 we can see the measurement is in good correspondence with the mechanical model for the respective type of breathing [3]. We can observe the following typical motions along individual axes:

x-axis (superio-inferior)

Bucket Handle (B): During inspiration the upper thorax (lines 1–2) moves in the superior direction along the x axis (in the negative direction) and the lower thorax (lines 3–4) moves even more in this direction. This corresponds to negative x entries.

Abdominal (A): There is very little motion in the upper and lower thorax during inspiration.

Pump Handle (P): Motions are similar to *bucket handle* type, except they are more pronounced in lower thorax.

y-axis (latero-lateral): Along this axis there should be no motion in either type of breathing. The lateral motions observed in our measurement were indeed very small and are omitted from the prototypes.

z-axis (posterio-anterior)

Bucket Handle: During inspiration the upper thorax moves forward and the abdominal wall backward. This corresponds to positive z entries on lines 1–4 and negative entries on lines 5–6.

Abdominal: During inspiration the thorax does not move. This corresponds to small z entries on lines 1–4.

Pump Handle: During inspiration both thorax and abdominal wall move forward. This corresponds to positive z entries on lines 1–5.

Note that the standard deviations are often comparable to the measurements itself and that their variations in magnitude are up to 1:3. It follows that any recognition of breathing type must take into account these deviations to weight data properly.

1.5 The BAP Index

From the normalized prototypic measurements a probabilistic model was created as follows. The 12 numbers per prototype $\lambda \in \{B, A, P\}$ (two rows in Tab. 1) define a vector $\mathbf{x}_\lambda$. For each prototypic class λ we construct a diagonal covariance matrix $\mathbf{S}_\lambda$ from the individual variances, ignoring the off-diagonal terms. Each prototype is then associated with probability distribution function

$$p(\mathbf{x} \mid \lambda) = \frac{1}{\sqrt{\det(2\pi\mathbf{S}_\lambda)}}\, e^{-\frac{1}{2}(\mathbf{x}-\mathbf{x}_\lambda)^\top \mathbf{S}_\lambda^{-1}(\mathbf{x}-\mathbf{x}_\lambda)}. \tag{6}$$

		line					
		1	2	3	4	5	6
B	x	-0.231 ± 0.054	-0.290 ± 0.043	-0.342 ± 0.038	-0.415 ± 0.041	-0.259 ± 0.035	-0.194 ± 0.046
	z	0.418 ± 0.067	0.420 ± 0.074	0.236 ± 0.095	0.052 ± 0.111	-0.054 ± 0.102	-0.015 ± 0.040
A	x	0.065 ± 0.044	0.072 ± 0.044	0.080 ± 0.049	0.022 ± 0.067	-0.025 ± 0.069	0.147 ± 0.114
	z	0.014 ± 0.150	0.004 ± 0.134	-0.007 ± 0.104	0.066 ± 0.106	0.579 ± 0.083	0.714 ± 0.082
P	x	-0.172 ± 0.050	-0.255 ± 0.045	-0.385 ± 0.041	-0.406 ± 0.045	-0.256 ± 0.037	-0.174 ± 0.031
	z	0.193 ± 0.108	0.337 ± 0.075	0.427 ± 0.043	0.340 ± 0.060	0.086 ± 0.043	-0.005 ± 0.031

Table 1: Prototypes for Bucket Handle (B), Abdominal (A), and Pump Handle (P) breathing patterns. The means and standard deviations are used to construct the BAP index. The rows in each type are the rows of the normalized matrix $\mathbf{X}$.

	BD 1	BD 2	BD 3	BN 1	BN 2
B	100	100	100	100	100
A	0	0	0	0	0
P	0	0	0	0	0
	AD 1	AD 2	AD 3	AN 1	AN 2
B	0	0	0	0	0
A	100	100	100	100	100
P	0	0	0	0	0
	PD 1	PD 2	PD 3	PN 1	PN 2
B	0	0	0	0	2
A	0	0	0	0	0
P	100	100	100	100	98

Table 2: BAP index for the training (xD) and test (xN) data.

This function gives the probability that (a new) measurement $\mathbf{x}$ belongs to class λ. The three posterior probabilities

$$p(\lambda \mid \mathbf{x}) = \frac{p(\mathbf{x} \mid \lambda)}{\sum_{\lambda \in \{B,A,P\}} p(\mathbf{x} \mid \lambda)} \tag{7}$$

for $\lambda \in \{B, A, P\}$ then represent the BAP index. The posterior probabilities are obtained from $p(\mathbf{x} \mid \lambda)$ by Bayes formula using equiprobable prior $P(\lambda) = \frac{1}{3}$ for all $\lambda \in \{B, A, P\}$.

The three numbers of the BAP index sum to unity. They represent the three probabilities that a given measurement belongs to the three respective classes. If the first number is the highest, the most probable breathing type is *bucket handle*. If the second number is the highest, the most probable breathing type is abdominal. Likewise, if the last number is the highest, the most probable type is *pump handle*. If the actual breathing pattern is a mixture of the prototypes, the three numbers represent the mixture.

To verify if the prototypes are sufficiently wide apart in the 12-dimensional space of the measurement, Tab. 2 shows the BAP indices for all nine training measurements used to construct the prototype along with six more measurements from the same subject. The prototypic measurements (xD) were taken under deep breathing but the six additional measurements (xN) were taken under normal breathing. The three probabilities are shown as percentages rounded to integer numbers. Thus BAP $= (100, 0, 0)$ is a clear *bucket handle* breathing type, BAP $= (0, 100, 0)$ is a clear abdominal breathing type and BAP $= (0, 0, 100)$ is a clear *pump handle* breathing type. We can see in Tab. 2 that the individual types were all recognized correctly, with great certainty.

2 Induced Breathing Types

We collected several measurements of breathing induced by various postures. The subject was the same as the one defining the prototypes. The postures are coded here as follows:

IN	normal posture, ideal normal breathing
ID	normal posture, ideal deep breathing
WON	weight resting on the outer sole edges, normal breathing
WOD	weight resting on the outer sole edges, deep breathing
WIN	weight on inner edge, normal breathing
WID	weight on inner edge, deep breathing

	IN	ID 1	ID 2	WON	WOD 1	WOD 2	WIN	WID 1	WID 2
B	100	100	100	97	76	100	100	100	92
A	0	0	0	0	0	0	0	0	0
P	0	0	0	3	24	0	0	0	8

	CEN	CED 1	CED 2	SN	SD 1	SD 2	S
B	1	99	33	100	7	99	88
A	0	0	0	0	0	0	0
P	99	1	67	0	93	1	12

Table 3: Recognition of posture-induced breathing on the same test subject. The numbers at the identificators are trials, e.g. in ID 2, means 2nd trial.

CEN	with chest extension, normal breathing
CED	with chest extension, deep breathing
SN	shoulder blades moving towards each other, normal breathing
SD	shoulder blades moving towards each other, deep breathing
S	with straightening during inspiration

The results are shown in Tab. 3. The ideal breathing was correctly recognized as *bucket handle.* We can see that the B–P transitions are more likely in the BAP index than the B–A or P–A. Indeed, the B and P prototypes are quite close to each other, see Tab. 1. The switches between B and P types in the CE and S sets may be related to the fact that the prototypes are very far from these breathing types, the probabilities $p(\mathbf{x} \mid \lambda)$ are small and recognition is unstable.

3 Results on Four Groups

We used the method described above to evaluate the success of breathing exercise. Results in this study are presented on three test groups and one test group. The test groups underwent breathing exercises, each individual was measured before the exercise program and after the program to quantify the change induced by the exercises. The program duration was different for the individual groups as shown by the following table:

group	participants	exercise programme duration	exercise intensity
L	7	4 weeks	1h, 3× per week
H	4	6 weeks	1h, 3× per week
A	8	6 weeks	1h, 3× per week

The control group did not perform any exercises. The two measurements were about 1 week apart in time.

Each of the three test groups were approximately homogeneous in age and had common occupational background. Both sexes were involved but most of the subjects were females.

Results for three test groups are shown in Tabs. 4–5 and results for the control group are shown in Tab. 6.

We can see that in the control group, the subject C8 changed breathing from *bucket handle* to abdominal.

If we consider *bucket handle* a better breathing type than abdominal type and abdominal type better than the *pump handle* type then the exercise improved breathing pattern in subjects L2, L8, L10, H5, A8. The breathing worsened in L6, H1, A3. In the rest of the subject it did not change.

	L2	L3	L4	L6	L8	L9	L10
	before						
B	0	100	100	93	95	0	97
A	0	0	0	0	0	100	0
P	100	0	0	7	5	0	3
	after						
B	100	100	100	61	100	0	100
A	0	0	0	0	0	100	0
P	0	0	0	39	0	0	0

	H1	H2	H4	H5
	before			
B	100	100	100	2
A	0	0	0	0
P	0	0	0	98
	after			
B	0	100	100	100
A	100	0	0	0
P	0	0	0	0

Table 4: Exercise results for groups L (left) and H (right).

	A1	A2	A3	A4	A5	A6	A8	A9
	before							
B	100	100	100	100	100	100	0	87
A	0	0	0	0	0	0	0	0
P	0	0	0	0	0	0	100	13
	after							
B	100	100	87	100	100	100	37	86
A	0	0	0	0	0	0	0	0
P	0	0	13	0	0	0	63	14

Table 5: Exercise results for group A.

	C1	C2	C3	C4	C5	C6	C7	C8
	1st measurement							
B	0	99	100	89	100	100	100	100
A	100	0	0	0	0	0	0	0
P	0	1	0	11	0	0	0	0
	2nd measurement							
B	0	100	100	100	100	100	100	0
A	100	0	0	0	0	0	0	100
P	0	0	0	0	0	0	0	0

Table 6: Results for the control group.

4 Discussion and Conclusions

The BAP index proposed in this report is our first successfull attempt to reliably quantify breathing type based on photogrammetric data. Our previous attempt to construct an index that recognizes breathing pattern were not successfull because of high variability caused by various external factors. The three-fold normalization (centers of gravity, suppression of the non-breathing component and normalization of the feature vector to unit length) suppresses the variability. Most importantly, the resulting index is able to recognize the breathing type without being excessively sensitive to the magnitute of the breathing movements, see Tab. 2.

Correlation with clinical examination is necessary to make any strong conclusions. Until then we cannot not attempt any medical interpretation of the results reported here.

The probability density for the prototypic classes obtained by the method seem rather narrow in the 12-D feature space. The side-effect of this is the poor ability of the index to capture breathing patterns that 'are in between' the three prototypic classes: the result seems almost always crisp. The generalization of the existing three-class classifier is thus poor. As a result, even small differences in measured data cause instability in repeated measurement, as seen in the results on the test set in Tab. 3, for instance. The percentage of *bucket handle* classifications in the three test set and in the control set is higher than expected. This behavior may be also related to the poor generalization.

On the other hand, narrow probability distrubutions suggest that discrimination of many different breathing types might be possible. Making the Gaussians (6) wider helps somewhat but is is difficult to select a suitable rule for the enlargement.

The method reported here relies on centers of gravity of the set of six horizontal lines. An open question remains the possibility to use the direct (48 dimensional) measurement. But high dimension could make the poor generalization even worse. The question then remains if a suitable projection method could work. For this, more prototypic measurements would be necessary.

Future work also includes using probability distribution more natural on points on a unit sphere.

To conclude, there is still room to improve the index, especially its generalization ability, which is the subject of our ongoing work.

References

[1] J. Čihák and R. Šára. A photogrammetric system for measuring breathing movements. Research Report CTU–CMP–2004–17, Center for Machine Perception, K13133 FEE Czech Technical University, Prague, Czech Republic, December 2005.

[2] G. Ferrigno, P. Carnevali, A. Aliverti, F. Molteni, G. Beulcke, and A. Pedotti. Three-dimensional optical analysis of chest-wall motion. *Journal of Applied Physiology*, 77(3):1224–1231, September 1994.

[3] I. A. Kapandji. *The Physiology of Joints*. Churchill Livingstone, London, 1975.